# Potential and limits of InSAR data for the reconstruction of buildings

U. Stilla, U. Soergel, and U. Thoennessen

***Abstract*-- The automatic reconstruction of buildings for the generation of city models is of great interest for different tasks. 3D information can be directly obtained from both, laser (LIDAR) and radar (InSAR) measurements. The data acquisition by SAR is described, with emphasis on the special properties of the interferometric SAR principle. A segmentation approach for building reconstruction is proposed. In case of InSAR special effects are taken into account, which are caused by the side-looking illumination. The estimation of the signal noise is considered in the segmentation process. Besides the elevation, the intensity information is exploited to detect building areas. The results show that building reconstruction is possible from InSAR, but the achievable level of detail cannot be compared with LIDAR. Inherent geometric constraints which limit the reconstruction of buildings from SAR data of dense urban areas are discussed.**

***Index Terms*--Image segmentation, Interferometry, Object recognition, Synthetic aperture radar.**

## I. Introduction

THREE-dimensional city models are of great interest for visualization, simulation and monitoring purposes in different fields. A typical application is the visualization of the influence of a planned building to the surrounding townscape for city and regional planning. Additionally, there is a growing demand for such models in civil and military mission planning. City models are used as basis for simulation e.g. in the fields of environmental engineering for microclimate investigations or telecommunications for transmitter placement. Furthermore, 3D information can be used for monitoring, e.g. damage assessment after an earth quake.

All the mentioned tasks require knowledge about the 3D structure of buildings. Besides the classical photogrammetric approaches to determine object heights indirectly, range sensors like LIDAR and interferometric SAR (InSAR) play an important role since recent years.

For topographic mapping data acquisition in nadir view is advantageous, especially in dense urban scenes with elevated objects. The LIDAR principle allows airborne applications in oblique (e.g. obstacle warning systems) and in nadir view as well. In contrast to LIDAR the SAR principle requires a side-looking illumination. LIDAR bases on the time-of-flight measurement of reflected infrared laser pulses, while InSAR exploits the phase difference of two measurements of the radar cross-section. Current laser systems achieve a higher accuracy compared to radar systems which are more sensitive to noise, because the measurement is based on a phase difference of two signals. Typically, the obtained accuracy is in the order of decimeter for LIDAR and about some meter for InSAR. LIDAR and InSAR are both active systems which illuminate the scene with electromagnetic waves and measure the backscattered signal component. Due to the different wavelengths (e.g. LIDAR: 1.5 µm, SAR: 3cm) special surface properties are sensed, because the reflectance depends on the surface roughness compared to the wavelength. Furthermore, different behavior concerning atmospheric attenuation and weather conditions are observed. While radar shows almost no sensitivity to weather influence, laser is attenuated from rain or fog and the signal might be reflected away from the sensor if the surface is covered with frost or ice. Another advantage of SAR is the opportunity to record large areas in a short time and from a large distance. Fig. 1 shows a SAR image from a section of the test area Karlsruhe (1 pixel = 1m x 1m).

Fig. 1. SAR image of test area Karlsruhe (City center, Castle and Campus)

Due to the mentioned features, both sensors are of interest for the generation of 3D descriptions [1]. For some applications, e.g. disaster management LIDAR data [2] as well as InSAR data [3] were evaluated. A fusion of LIDAR and InSAR data of vegetated areas was proposed by Slatton et al. [4]. In case of dense urban areas for a fusion of man-made objects of both datasets a building reconstruction is advantageous. For such a building reconstruction the sensor principle has to be considered. A crucial step for the generation of 3D-vector descriptions of buildings is the

U. Stilla, U. Soergel and U. Thoennessen are with the FGAN-FOM Research Institute for Optronics and Pattern Recognition, 76275 Ettlingen, Germany (e-mail: usti@fom.fgan.de, soe@fom.fgan.de, thoe@fom.fgan.de).

0-7803-7059-7/01/$10.00 © 2001 IEEE

segmentation of the elevation data. In this paper we focus on the segmentation of InSAR data for the reconstruction of buildings, with emphasis on the sensor properties of SAR.

## II. Elevation Data From Radar

### A. Acquisition of SAR data

The moving sensor illuminates the scene with microwaves in a side-looking manner. The signal is partly either reflected away from the sensor or scattered towards the sensor, depending on the roughness of the scene compared to the signal wavelength. Hence, the choice of the sensor wavelength (e.g. X-band: 3cm, P-band: 64cm) depends on the task. The improved ground resolution of current systems suggests to employ this sensor for the analysis of man-made objects. But, due to specific SAR effects, this imagery is difficult to interpret. Particularly in urban areas, phenomena like layover, shadow, multi-path signals and speckle [5] have to be considered.

Some of the phenomena are illustrated in Fig. 2. Let us assume that a building is sensed in a side looking manner from point F. In the slant range image IS the points A, B, C appear according to their distance. Hence, the point A of the building footprint appears as A' behind point B' and in-between B' and C'. The area in-between B'A' is called layover area. Layover occurs always at vertical building walls facing towards the sensor. It leads to a mixture of signal contributions from the building and the ground in the SAR image, because the elevated objects are closer to the sensor than the ground. The slant image (see Fig. 5a) shows a geometic distortion in range direction which makes an object recognition and interpretation more difficult. Hence, for image interpretation the data are sampled to a rectabgular grid on the ground (Fig. 6a). However, the order of the points B", A", C" in the ground image is still the same as in the slant image.

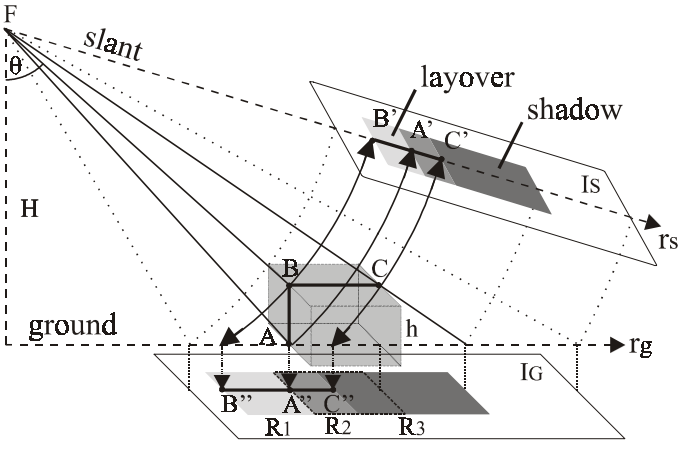


Fig. 2. Projection of a building into slant image IS and ground image IG.

On the other side the building casts a shadow which occludes smaller objects behind and appears dark in the image. However, the height of a detached building can be derived from the shadow length and the viewing angle. Both effects are visible at the high building located on left of Fig. 3. The scene is illuminated from left. Due to the elevation the building appears shifted towards the sensor, covering partly a smaller building. Additionally, a building is partly occluded from the shadow cast by the high building.

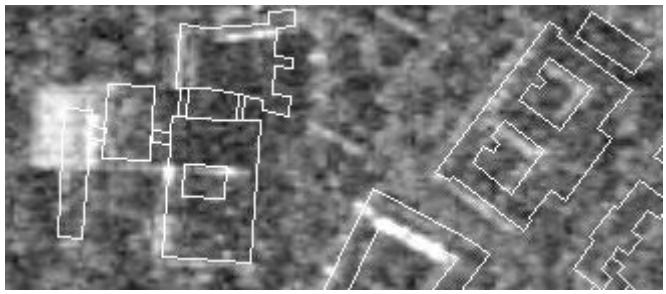

Fig. 3. Scene detail in ground range overlaid with the layer BULDING of the vector map. Range direction from left to right.

### B. Interferometric SAR principle

SAR interferometry takes benefit from the coherent SAR measurement principle. Fig. 3 illustrates the principle of airborne single-pass across-track interferometry measurement. Two antennas are mounted above each other on the carrier with geometric displacement B. One of the antennas illuminates the scene and both antennas receive the backscattered complex signals.

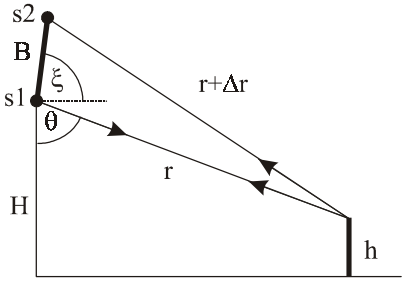


Fig. 4. SAR system AER II and geometry of across-track interferometry.

The interferogram S is calculated by a pixel by pixel complex multiplication of the master signal $s_1$ with the complex conjugated slave signal $s_2$. Due to the baseline B, the distances from the antennas to the scene differ by Δr, which results in a phase difference Δφ in the interferogram:

$$S = s_1 \cdot s_2^* = a_1 \cdot e^{j\varphi_1} \cdot a_2 \cdot e^{-j\varphi_2} = a_1 \cdot a_2 \cdot e^{j\Delta\varphi}$$
$$with \quad \Delta\varphi = -\frac{2\pi}{\lambda}\Delta r \tag{1}$$

The phase difference Δφ is unambiguous in the range ]- π,π] only. Thus, a phase-unwrapping step is often required before further process. Furthermore, the range dependency of Δφ has to be removed (flat earth correction). Afterwards, the elevation differences Δh in the scene can be derived from Δφ:

$$\Delta h = \frac{\lambda}{2\pi} \cdot \frac{r \cdot \sin(\theta)}{B \cdot \cos(\xi - \theta)} \cdot \Delta\varphi, \tag{2}$$

with parameters distance r, wavelength λ, antenna geometry angle ξ and viewing angle θ. The standard deviation of the interferogram phase depends approximately on the SNR and the number of independent looks L:

$$\sigma_\varphi \approx 1/\left(\sqrt{SNR} \cdot \sqrt{L}\right) \tag{3}$$

With Equations 2 and 3, finally the standard deviation of the elevation is obtained:

$$\sigma_h \approx \frac{\lambda}{2\pi} \cdot \frac{r \cdot \sin(\theta)}{B \cdot \cos(\xi - \vartheta)} \cdot \frac{1}{\sqrt{SNR} \cdot \sqrt{L}}. \tag{4}$$

The coherence γ is a function of the noise impact of the interferogram. It is usually estimated from the data by the magnitude of the complex cross-correlation coefficient of the SAR images:

$$\hat{\gamma} = \frac{\left|\sum_{n=1}^{N} s_1^{(n)} \cdot s_2^{(n)*}\right|}{\sqrt{\sum_{n=1}^{N} \left|s_1^{(n)}\right|^2 \cdot \sum_{n=1}^{N} \left|s_2^{(n)}\right|^2}} \approx \frac{1}{1 + \frac{1}{SNR}} \tag{5}$$

Hence, the local quality of an InSAR DEM can be directly assessed from the data by the related coherence value. Furthermore, the coherence is exploited for change detection tasks: changes in the period between repeated SAR measurements lead to decorrelation of the signals.

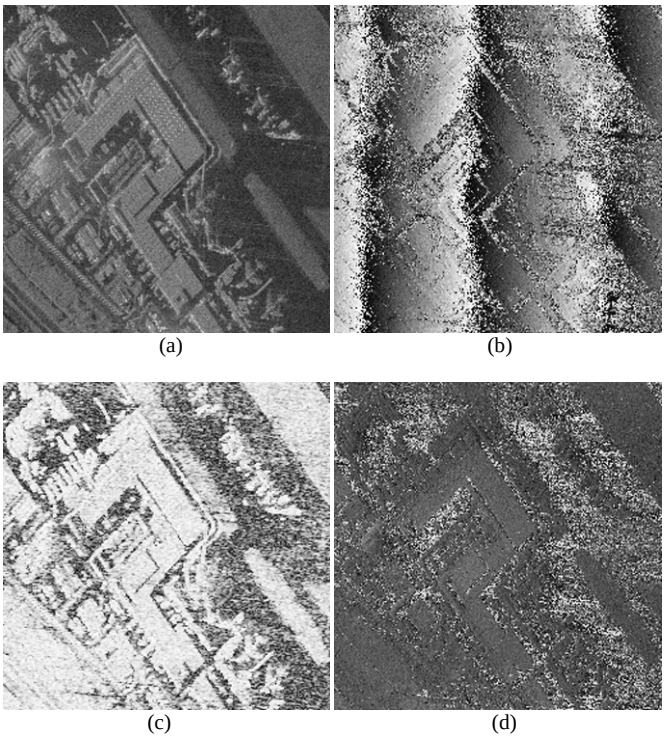

(a) (b) (c) (d)

Fig. 5. Slant images of test area Frankfurt. a) intensity, b) phase diffference, c) coherence, d) elevation

## III. SEGMENTATION OF INSAR DATA

As mentioned above, the elevation is derived from the difference phase of the interferogram. Especially in areas with low SNR - respectively poor coherence - the phase information is disturbed. Hence, the noise component has to be removed or at least reduced before further analysis. Often the noise is decreased by averaging, e.g. low-pass filtering or multi-look processing. However, this leads to reduced spatial resolution and blurred phase jumps at object boundaries.

Other methods base on statistical modeling of sensor and scene [6]. With bayesian inference the data is restored to a configuration which most probably caused the measured data [7]. Scene and sensor are modeled according to the central limit theorem, which requires a large number of independent scatterers per resolution cell, contributing each a small impact to the measured signal only. In case of urban areas this assumptions do not hold anymore, because of the presence of dominant scatterers, the privileged rectangular alignment of the objects and multi-path signals [8]. Furthermore, the number of scatterers per resolution cell decreases the higher the resolution of the sensor becomes. Thus, in urban areas the data cannot be restored without additional knowledge about the scene.

Recently, approaches for building reconstruction in InSAR elevation data were proposed, which either apply model-based machine-vision methods [1] or take typical phenomena into account, like layover and shadowing [9]. These methods base on the analysis of the geocoded DEM alone.

In our approach the entire set of complex InSAR data (phase, intensity and coherence) is analyzed for the segmentation of extended buildings.

### *A. Assumptions for the model based segmentation*

We assume that man-made objects like buildings have often right-angled structures and appear in the intensity image as regions with similar intensity. The edges of these objects are visible in the intensity image. Building walls are assumed as vertical. The elevation of buildings pixels differs significantly from ground pixels. Roof parts of buildings are assumed as to be flat. They can be described by prismatic models. Detached vertical building faces which are facing towards the sensor leads to areas of bright intensity caused by layover and multi-path effects. At the other building side shadow areas with low intensity and poor coherence occurs caused by occlusion.

### *B. Segmentation in the interferogram*

In a pre-processing step the intensity data is despeckled and the elevation information is smoothed by median filtering. The initial segmentation is carried out by a combined region growing in the intensity and the elevation data [12]. It is crucial to detect as many object boundaries as possible. Hence, the adaptive region growing threshold is set to a small value. As a consequence, over-segmentation occurs, which is corrected in a subsequent post-processing step.

*1) Generation of a depth map considering the SNR*

For each segment a height is calculated considering the SNR. The coherence is used as weighting factor for averaging the elevation values in this smoothing step. The results in a preliminary depth map of prismatic objects. Segments with low average intensity and coherence are regarded as unreliable. These segments are assumed to coincide with shadow areas or roads and are considered later to check the consistency of the results.

*2) Detection of buildings*

Mayor building parts and minor building parts (superstructures) are discriminated. Minor building parts are surrounded by mayor building parts. Adjacent building parts are joint. If an object matches the model with respect to area, shape and compactness, then it is labeled as a building .

Shadow cast from a rectangular building part leads to either long or L-shaped segments, depending on the aspect. Their width is a function of viewing angle and object elevation. Hence, for each building candidate an expectation area for a shadow stripe is predictable. Unfortunately, shadow cannot always be distinguished from objects which appear similar in the data, like roads. Therefore, as a minimum requirement, an area of the set of unreliable segments is expected to be found at the predicted shadow location. If so, the candidate segment is labeled to be a building. In case shadow does not interfere with roads, a more subtle analysis is carried out. Shadow stripes are extracted in the intensity data with a simple structural image analysis algorithm. Starting with short lines as primitives, stripes are built-up, which enclose regions of low intensity.

### C. Post-processing

Shadow areas are used to overcome under-segmentation. Segments which contain a possible shadow area are further investigated [12]. The under-segmentation is corrected in two different ways. If the histogram of the original height values shows a bimodal curve, the segment is split in two closed segments, if possible. In a second approach a region growing step in the median filtered heights is performed. In contrast to the initial segmentation, the border towards the shadow region is used as seed [10] and the threshold is smaller. Over-segmentation is corrected by merging adjacent segments with similar heights. After post-processing the depth map is recalculated.

### D. Results

Our test data were acquired with the airborne AER-II sensor of FGAN [11]. Fig. 6a shows the intensity image (ground range) of a scene section of Frankfurt airport. The range direction is from left to right, ground resolution is approximately one meter. Several extended buildings are present in the scene at the airport Frankfurt. The rooftops are generally flat with small elevated superstructures, mostly required for illumination and air-conditioning inside the building. Fig 6b shows the segmentation result, which is visualized in 3D in Fig. 6c.

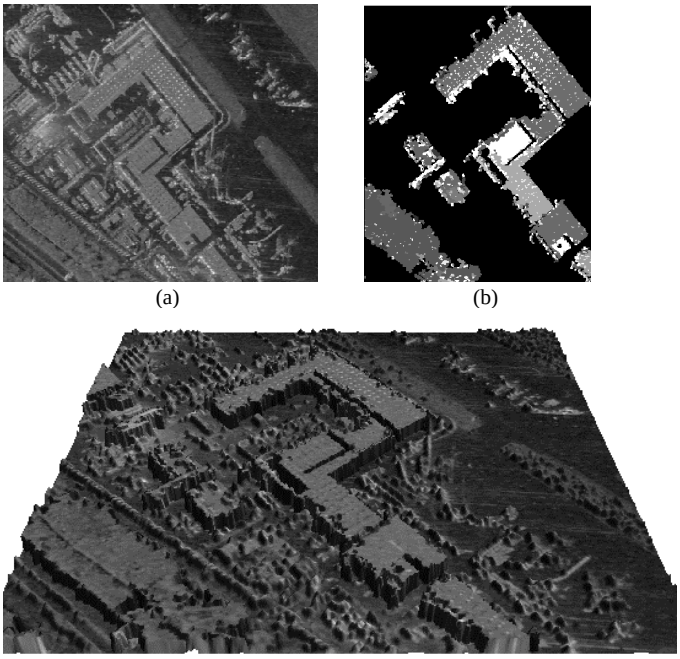

(a) (b) (c)

Fig. 6. Test area Frankfurt: a) intensity, b) segmentation, c) 3d visualization.

## IV. Discussion

It was shown that in InSAR data a segmentation of building structures is possible. The InSAR test dataset Frankfurt contained large and detached buildings with flat roofs. Extended building parts with different height could be distinguished by the segmentation approach. Due to the noisy nature of the InSAR elevation data, the achieved level of detail was not comparable with results from LIDAR [13],[14].

Additionally, the reconstruction of man-made objects in dense urban areas from SAR imagery is limited by inherent geometric constraints. As shown in Fig. 2, layover (Area R1) leads to a signal mixture from ground and building (wall and roof), in contrast to area R2, which origins from the roof only. The width (A"C") of area R2 depends on angle $\theta$ and the building geometry w and h. R2 disappears if $h = w \tan \theta$ when the point C falls together with point A on the ground (Fig. 7a). That means, if $h = w \tan \theta$ a proper roof reconstruction is not possible anymore. As a consequence, for building reconstruction a large viewing angle $\theta$ is advantageous. However, a large $\theta$ leads to extended shadow regions behind buildings, which might occlude a lower building or street of width $s = h \tan \theta$ (Fig. 7b). Furthermore, the area of unreliable image data may be extended from layover l caused by buildings located at the other side of the street, as depicted in Fig. 7c. Additionally, roofs with perpendicular orientation towards the sensor cause total reflections and strong signal responses (Fig. 7d). Corners, antennas and sloped rooftops may lead to strong signal responses due to multi-bounce effects, respectively perpendicular orientation towards the sensor, depending on the aspect (e.g. at the circle around the castle in Fig. 1). At building walls multi-path propagation of signals occurs, which leads to a wrong range.

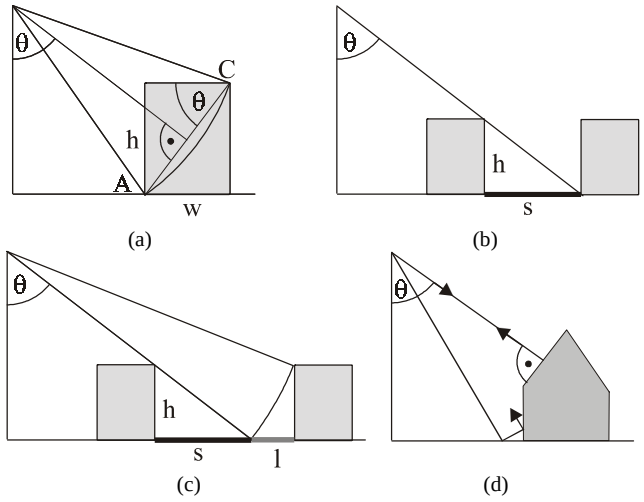


Fig. 7. Geometric constraints for the acquisition of SAR images from buildings.

The smoothed InSAR elevation data can be used for change detection purposes, at least for extended buildings. But the results indicate that the approach is limited to course scene descriptions only. For image based detail analysis, like roof reconstruction, the data is still too inaccurate. If a further improvement of the accuracy is achievable more sophisticated object models become appropriate in the future.

The segmentation results might be used to correct the geometric displacement of the buildings. Furthermore, they could be incorporated in a refined phase unwrapping step in which shadow and layover areas are masked.

The radar illumination aspect is important, because of the phenomena mentioned above. Hence, the data acquisition of certain areas of the urban scene may be optimized by a simulation of SAR phenomena [15]. A suitable basis for such a simulation is a 3D city model, which can be obtained from LIDAR data.

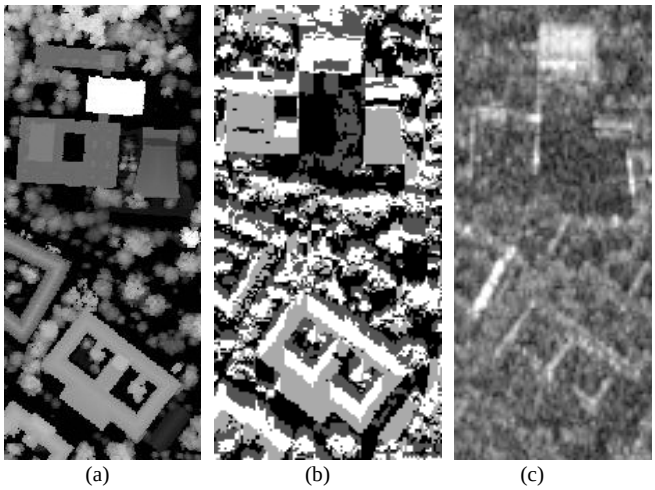


Fig. 8. a) Laser elevation data, b) SAR phenomena image, c) SAR image

In Fig. 8a such LIDAR data of a section of the test area Karlsruhe (University campus) is shown. The DEM is incorporated to predict geometric phenomena for an illumination from above with a view angle $\theta=32°$. Layover is depicted in white, shadow in black. Areas with a mixture of layover and shadow appear dark gray. The region of the scenes which is expected to lead to undisturbed signal is shown in bright gray. In Fig. 8c the corresponding section of the SAR image which was acquired from the simulated position is depicted for comparison.

## ACKNOWLEDGMENT

We want to thank Dr. Ender (FGAN-FHR Research Institute for High Frequency Physics and Radar Techniques) for providing us the InSAR data (AER II).

## REFERENCES

[1] Gamba, P., Houshmand, B. 2000. Digital surface models and building extraction: A comparison of IF-SAR and LIDAR data. IEEE Trans. on Geoscience and Remote Sensing 38(4): 1959-1968.

[2] Kakumoto, S., Hatayama, M., Kameda, H., Taniguchi, T. 1997. Development of disaster management spatial information system. Proc. GIS'97 Conf., 595-598.

[3] Takeuchi, S., Suga, Y., Yonezawa, C., Chen, C.H. 2000. Detection of urban disaster using InSAR - a case study for the 1999 great Taiwan earthquake. Proc. IGARSS 2000 (on CD ROM).

[4] Slatton, K.C., Crawford, M.M., Evans, B.L. 2000. Combining interferometric radar and and laser altimeter data to improve estimates of topography. Proc. IGARSS 2000 (on CD ROM).

[5] Schreier, G. 1993. Geometrical properties of SAR images. In G. Schreier (ed.), SAR geocoding: data and systems: 103-134. Karlsruhe: Wichmann.

[6] Lee, J.S., Hoppel, K.W., Mange, S.A., Miller, A.R. 1994. Intensity and Phase Statistics of Multilook Polarimetric and Interferometric SAR Imagery. IEEE Trans. on Geoscience and Remote Sensing 32(5): 1017-1028.

[7] Walessa, M., Datcu, M. 2000. Enhancement of interferometric DEMs by spatially adaptive model-based filtering in non-stationary noise. Proc. EUSAR, 695-698.

[8] Meyer, R.H., Roy R.J. 2000. Algorithms for interpreting SAR imagery of complex building scenes. In Zelnio, E. (ed.), Algorithms for synthetic aperture radar imagery VII, SPIE Proc. vol. 4053, 642-651.

[9] Bolter, R., Leberl, F. 2000. Phenomenology-based and interferometry-guided building reconstruction from multiple SAR images. Proc. EUSAR, 687-690.

[10] Hoepfner, K.B. 1999. Recovery of Building Structure from IFSAR-Derived Elevation Maps. Technical Report 99-16, Computer Science Department, University of Massachusetts, Amherst.

[11] Ender, J.H.G. 1998. Experimental results achieved with the airborne multi-channel SAR system AER-II. Proc. EUSAR'98, 315-318.

[12] Soergel, U., Thoennessen, U., Gross, H., Stilla, U. 2000. Segmentation of interferometric SAR data for building detection. International Archives of Photogrammetry and Remote Sensing, vol. 33, part B1, 328-335.

[13] Stilla, U., Jurkiewicz, K. 1999. Reconstruction of building models from maps and laser altimeter data. In: Agouris, P., Stefanidis, A. (eds.), Integrated spatial databases: Digital images and GIS: 34-46. Berlin: Springer.

[14] Stilla, U., Soergel, U., Jaeger, K. 2000. Generation of 3D-city models and their utilisation in image sequences. International Archives of Photogrammetry and Remote Sensing, vol. 33, part B2, 518-524.

[15] Meier, E., Frei, U., Nuesch, D. 1993. Precise terrain corrected geocoded images. In G. Schreier (ed.), SAR Geocoding: Data and Systems: 173-185. Karlsruhe: Wichmann.